

# Boronate Ester Bullvalenes

Harshal D. Patel,<sup>a</sup> Thanh-Huyen Tran,<sup>a</sup> Christopher J. Sumbly,<sup>a</sup> Lukáš F. Pašteka,<sup>b</sup> and Thomas Fallon<sup>a\*</sup>

[a] Department of Chemistry, The University of Adelaide, Adelaide, SA 5005 (Australia)

[b] Department of Physical and Theoretical Chemistry, Faculty of Natural Sciences, Comenius University, Ilkovičova 6, Bratislava, Slovakia

\*Corresponding author: [thomas.fallon@adelaide.edu.au](mailto:thomas.fallon@adelaide.edu.au)

**ABSTRACT:** Boronate ester bullvalenes are now accessible in two to four operationally simple steps. This unlocks late-stage diversification through Suzuki cross-coupling reactions to give mono-, di-, and tri-substituted bullvalenes. Moreover, a linchpin strategy enables pre-programmed installation of two different substituents. Analysis of solution phase isomer distributions and single crystal X-ray structures reveals that isomer preference in the crystal lattice is due to general shape selectivity.

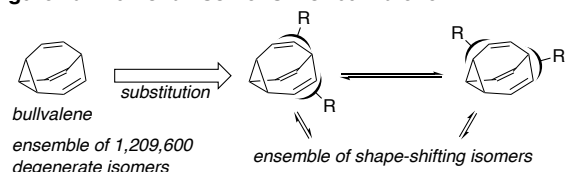
During the golden age of hydrocarbon chemistry, fluxional caged structures were discovered and intently studied.<sup>1</sup> The canonical examples are bullvalene,<sup>2</sup> semi-bullvalene,<sup>3</sup> and the barbaryl cation.<sup>4</sup> These remarkable molecular systems exist in a constant state of metamorphosis and defy traditional notions of chemical bonding and structure. Bullvalene is extraordinary as the only stable organic structure with the property of *total degeneracy*. Through an endless succession of Cope rearrangements all ten positions in the molecule exchange with every other, and there are no permanent carbon-carbon bonds. For substituted bullvalenes, substituents will spontaneously explore all possible relative arrangements and exist as a dynamic ensemble of isomers (Figure 1a).

For such an intriguing molecular scaffold, the synthetic methods available to prepare and modify derivatives are surprisingly limited.<sup>5</sup> Schröder first prepared the parent hydrocarbon in 1963 through a serendipitous two-step sequence from cyclooctatetraene (COT).<sup>6</sup> While this method was scalable, it had no versatility and further substitution was only achieved through low-yielding bromination/elimination sequences (Figure 1b).<sup>7</sup>

Recently, Echavarren reported the preparation of mono- and di-substituted bullvalenes using a modular gold-catalysed oxidative cyclisation as the key step (Figure 1c).<sup>8</sup> In a series of reports, Bode demonstrated the synthesis of highly complex tetra-substituted bullvalenes. (Figure 1d).<sup>9</sup> However, this approach required relatively long synthetic sequences.

This revival of interest in shape-shifting molecules is accompanied by a recognition of their potential in the context of dynamic covalent chemistry and molecular devices.<sup>10</sup> The foremost demonstration of these concepts is Bode's use of a tetrasubstituted bullvalene as a dynamic molecular sensor array for polyols.<sup>11</sup> However, further advances in this field demand more efficient synthetic methods.

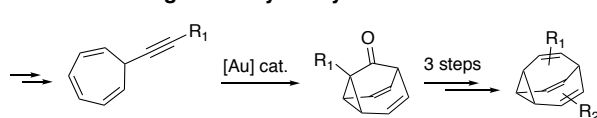
**Figure 1a. Fluxional isomerism of bullvalene**



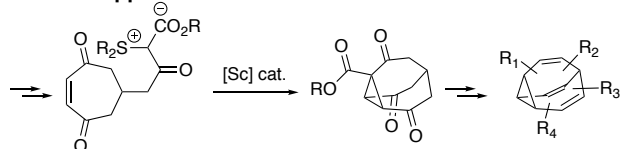
**1b. Schröder's synthesis of substituted bullvalenes**



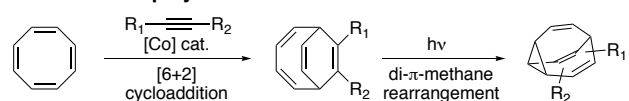
**1c. Echavarren's gold-catalysed synthesis of bullvalenes**



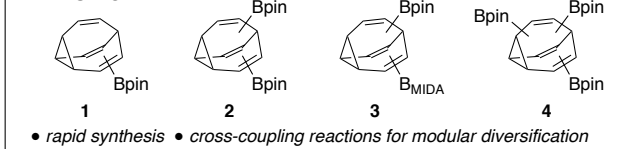
**1d. Bode's approach to tetrasubstituted bullvalenes**



**1e. Our two-step synthesis of substituted bullvalenes**



**1f. This work**



We recently reported a two-step approach to mono- and di-substituted bullvalenes through [6+2] cycloaddition of COT to alkynes followed by di- $\pi$ -methane rearrangement (Figure 1e).<sup>12</sup> While this represents the short-

est synthetic strategy to date, the substrate scope with respect to both reaction steps was admittedly limited. We recognised the overarching need for synthetic building blocks and methodology that would allow for the modular late-stage incorporation of desired substituents through versatile and reliable chemistries. Boronate ester functionalised bullvalenes became irresistible targets.

In this communication we report the efficient synthesis of a family of mono- di- and tri-substituted boronate ester bullvalenes **1-4** (Figure 1f) and demonstrate their general utility in Suzuki cross-coupling reactions. The disubstituted bullvalene **3** incorporates a pinacol boronate ester (Bpin) as well as *N*-methyliminodiacetic acid boronate ester (B<sub>MIDA</sub>) group. This linchpin enables selective double Suzuki cross-coupling reactions. The unparalleled versatility of this toolbox opens the way to explore shape-shifting chemical behaviour in a wide range of settings.

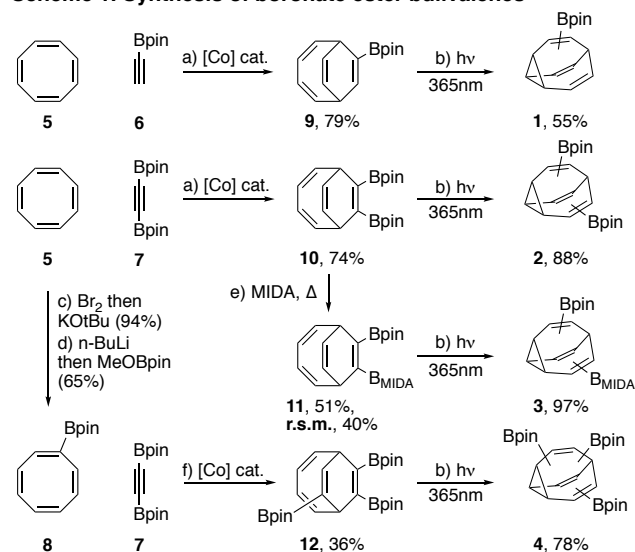
Suzuki cross-couplings gave access to a series of aryl substituted bullvalenes, many of which are highly crystalline. This allows for a comparative analysis of isomer preference in solution and the solid state. Solution phase population distributions were characterised through low-temperature NMR experiments and compared with the results of density functional theory (DFT) calculations. The isomer population distributions follow generally predictable lines. Single crystal X-ray analyses reveal several examples whereby a minor solution phase isomer is preferred in the crystal through what appears to be shape-selective crystallisation phenomena. This is supported by computational analysis of the crystal structures which indicates no specific intermolecular interactions are dictating the crystal packing.

The key to our synthetic strategy is the cobalt-catalysed [6+2] cycloaddition of alkynes with COT.<sup>13</sup> This catalytic system has emerged in the past two decades as a powerful and versatile tool.<sup>14</sup> Among the pioneering contributions of Hilt are several examples of [4+2] cycloaddition reactions involving alkynyl boronate esters.<sup>15</sup> This encouraging precedent suggested that mono-Bpin-acetylene **6** and bis-Bpin-acetylene **7**<sup>16</sup> might be good reaction partners in [6+2] cycloadditions with cyclooctatetraene. Happily, this turned out to be true providing access to the corresponding bicyclo[4.2.2]deca-2,4,7,9-tetraenes (BDT) **9** and **10** in good yield and on gram scale (Scheme 1). COT-Bpin **8**, prepared in two steps, undergoes [6+2] cycloaddition with **7** to give reliable access to the tri-Bpin-BDT **12**, albeit in low yield.<sup>17</sup> Bis-Bpin-BDT **10** was modified by condensation with *N*-methyliminodiacetic acid to give the corresponding ester **11**.<sup>18</sup>

With this range of boronate ester BDTs in hand we were delighted to find that the photochemical di- $\pi$ -methane rearrangement proceeded smoothly to give the corresponding bullvalenes in good to excellent yields. The use of inexpensive and operationally simple 365 nm

LED lamps together with 9*H*-thioxanthen-9-one as a triplet sensitizer renders this transformation particularly rapid and convenient.<sup>19</sup>

**Scheme 1. Synthesis of boronate ester bullvalenes<sup>a</sup>**



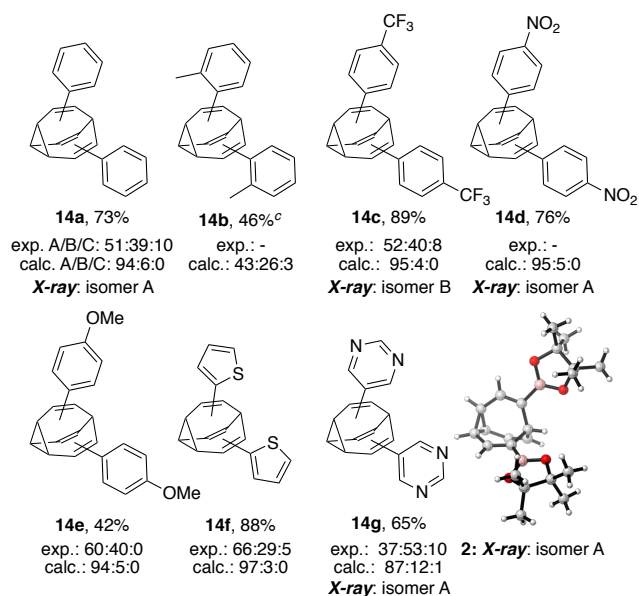
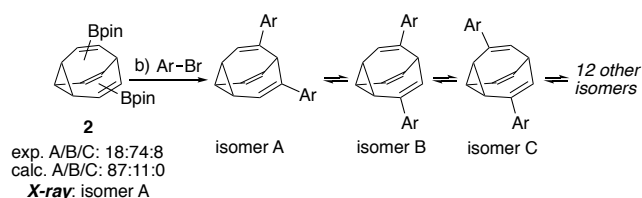
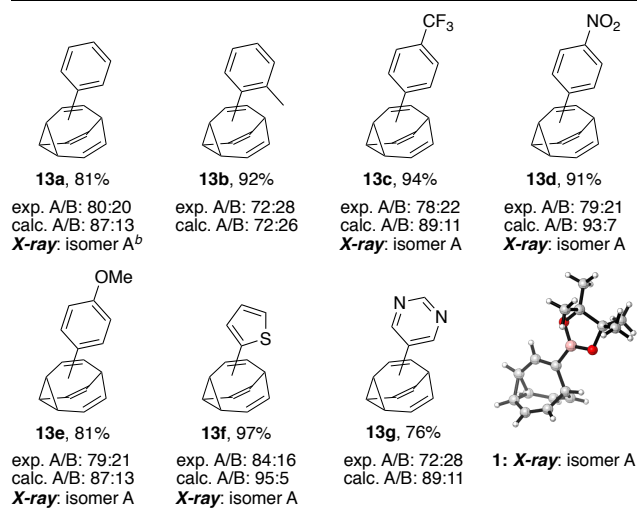
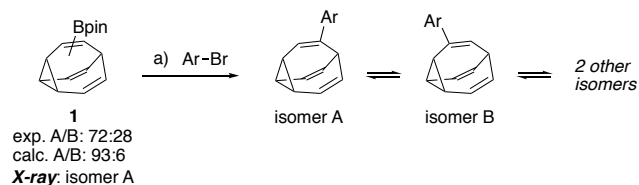
<sup>a</sup>Reagents and conditions: (a) alkyne (1.0 eq), CoBr<sub>2</sub>(dppe) (10 mol%), ZnI<sub>2</sub> (20 mol%), Zn (30 mol%), DCE, RT. (b) 9*H*-thioxanthen-9-one (1 mol%), THF, 365nm LED lamp, RT. (c) Br<sub>2</sub> (1.0 eq), KOtBu (1.0 eq), THF, -78 °C. (d) *n*-BuLi (1.0 eq), MeOBpin (1.0 eq), THF, -78 °C to RT. (e) MIDA (12.0 eq), DMSO, 120 °C, 8 hours. (f) alkyne (1.0 eq), CoBr<sub>2</sub>(dppe) (50 mol%), ZnI<sub>2</sub> (100 mol%), Zn (150 mol%), DCE, RT.

With this collection of boronate ester bullvalenes in hand we set out to demonstrate their ease of use in Suzuki cross-coupling reactions.<sup>20</sup> Mono-Bpin-bullvalene **1** couples with a range of aryl bromides to give the corresponding bullvalenes **13a-g** in good to excellent yields under simple and traditional catalytic conditions (Scheme 2a). Bis-Bpin-bullvalene **2** couples with bromo arenes to give diarylbullvalenes **14a-g** under identical reaction conditions (Scheme 2b).

MIDA boronate esters have emerged as excellent boronic acid masking group leading to effective linchpin cross-coupling strategies.<sup>21</sup> In the case of Bpin-B<sub>MIDA</sub>-bullvalene **3**, the reactivity of the Bpin and B<sub>MIDA</sub> groups can be cleanly differentiated with exclusive mono-coupling with *p*-bromobenzotrifluoride to give **15** in excellent yield (Scheme 3a). This was followed by a second coupling with a small range of aryl bromides to give differentially substituted diarylbullvalenes **16a-c** (Scheme 3b). This strategy opens up a wide range of possibilities for the targeted synthesis of fluxional molecules.

Tri-Bpin-bullvalene **4** underwent coupling with bromobenzene under somewhat more forcing Suzuki coupling conditions, but cleanly furnished triphenylbullvalene **17** in 71% yield (Scheme 3c). Triphenylbullvalene was previously prepared by Schröder and known to display intriguing dynamic behaviour.<sup>22</sup> In solution the major populated isomer is isomer B. However, recrystallisation gives exclusively the C<sub>3</sub> symmetric isomer A, as

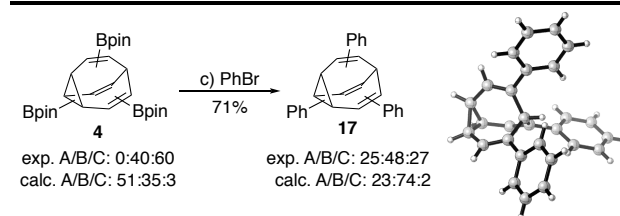
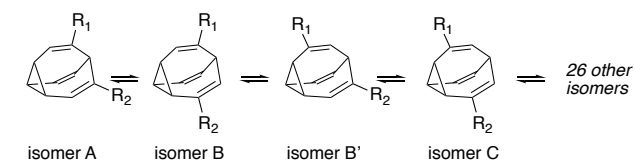
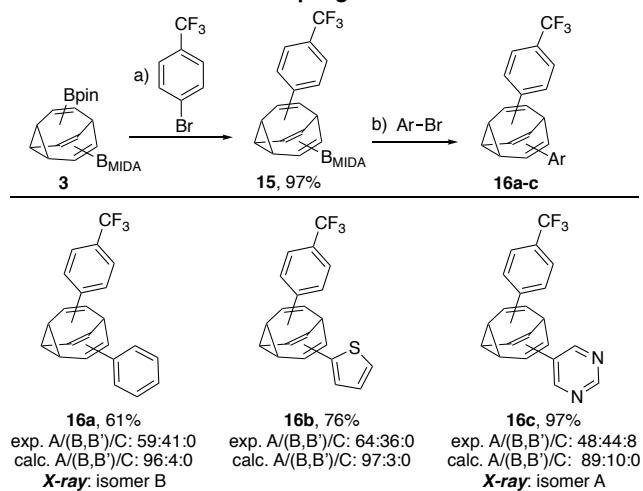
## Scheme 2. Suzuki cross-coupling of bullvalenes 1 and 2<sup>a</sup>



<sup>a</sup>Reagents and conditions: (a) Ar-Br (1.1 eq), Pd(PPh<sub>3</sub>)<sub>4</sub> (5 mol%), NaOH(aq), THF, 60 °C. (b) Ar-Br (2.2 eq), Pd(PPh<sub>3</sub>)<sub>4</sub> (5 mol%), NaOH(aq), THF, 60 °C. Single-point DFT calculations performed at B3LYP-D3BJ/Def2-TZVPPD/CPM solvent (chloroform) in Orca. <sup>b</sup>See ref 26. <sup>c</sup>2-iodotoluene used in place of 2-bromotoluene.

confirmed by single crystal X-ray analysis. Isomer A is also kinetically metastable with an experimentally determined room-temperature solution half-life of 1h.<sup>22</sup> The origin of this kinetic feature was explored in a recent study by our laboratory and traced to high barriers in the first and second generation isomerisation from isomer A.<sup>23</sup> DFT analysis and kinetic modelling of triphenylbullvalene predict an isomer A half-life of 4.5 min (see SI for full details).

## Scheme 3. Suzuki cross-coupling of bullvalenes 3 and 4<sup>a</sup>



<sup>a</sup>Reagents and conditions: (a) p-bromobenzotrifluoride (1.1 eq), Pd(PPh<sub>3</sub>)<sub>4</sub> (5 mol%), Ag<sub>2</sub>CO<sub>3</sub> (1.5 eq), THF, 60 °C. (b) Ar-Br (1.1 eq), Pd(PPh<sub>3</sub>)<sub>4</sub> (5 mol%), NaOH(aq), THF, 60 °C. (c) Ph-Br (3.3 eq), Pd(PPh<sub>3</sub>)<sub>4</sub> (10 mol%), NaOH(aq), THF, 80 °C. Single-point DFT calculations performed at B3LYP-D3BJ/Def2-TZVPPD/CPM solvent (chloroform) in Orca.

The solution phase isomer population distributions of most of the bullvalenes prepared herein was experimentally determined using low temperature NMR measurements.<sup>24</sup> Population distributions follow predictable patterns. Substituents generally prefer the olefinic positions, with a slight preference for the positions adjacent to the bridgehead. A DFT survey of relative stabilities was conducted employing our previously reported methods.<sup>12</sup>

The experimental and computational ratios are expressed as A:B, A:B:C, or A:(B,B'):C patterns (Schemes 2-4). The results are in excellent agreement with experiment for monosubstituted bullvalenes. For di- and tri-substituted bullvalenes agreement with experiment is good, but calculations tend to somewhat overestimate the stability of isomer A.

Diarylbullvalenes exist as dynamic ensembles of 15 isomers (homogeneous substituents) or 30 isomers (heterogeneous substituents), respectively. However, most of their time is spent within the A:B:C set of favoured isomers. Network analysis of diphenylbullvalene **14a** exemplifies this character (Figure 2). The network graph represents nodes as isomers and edges as transitions structures; all colour coded according to calculated relative energy. The A:B:C set of isomers are closely interconnected through a low energy isomerisation path and will be in rapid equilibrium at ambient temperature.

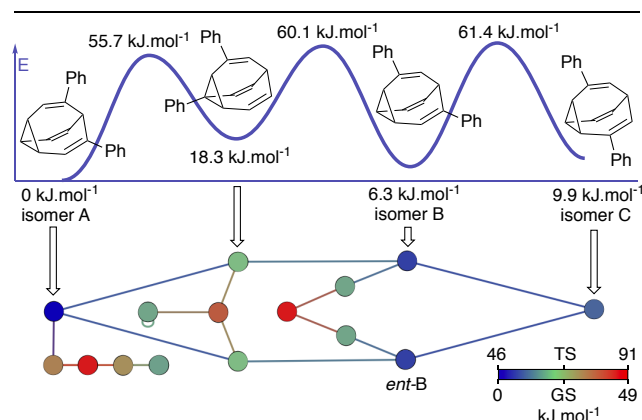


**Figure 2.** Network analysis of diphenylbullvalene **14a**: Single-point DFT calculations performed at B3LYP-D3BJ/Def2-TZVPPD/CPCM solvent (chloroform) in Orca.

McGonigal recently reported a study on the crystallisation behaviour of substituted *barbaralanes* – shape-shifting hydrocarbons that exist as bistable dynamic ensembles.<sup>25</sup> Detailed analysis using a range of experimental and computational techniques led to the conclusion that crystallisation into a minor barbaralane solution phase isomer is due to general shape-selectivity rather than specific non-covalent interactions. Similar phenomena seem to play out herein for aryl substituted bullvalenes.

Single-crystal X-ray structures were obtained for bullvalenes **1**, **2**, **13c**, **13d**, **13e**, **13f**, **14a**, **14c**, **14d**, **14g**, **16a**, **16c**, **17**, and **18** (selection shown in Figure 3a). For the mono-substituted bullvalenes, all compounds except **18** crystallise as the major solution phase isomer A.<sup>26</sup> Similarly, most disubstituted bullvalenes crystallise in their major solution phase isomer. However, for bis-Bpin-bullvalene **2**, aryl disubstituted variants **14c**, **14g**, **16a**, and the trisubstituted **17**, the inherent thermodynamic preference is overturned, and crystallisation gives a minor solution isomer.<sup>27</sup>

Diarylbullvalenes **16a** and **16c** provide an intriguing comparison. They are structurally very similar, differing only in the exchange of a phenyl group with a pyrimidine group, and would be expected to adopt nearly identical shapes. **16c** follows the solution preference and recrystallises into the V-shaped isomer A in which the pyrimidine group of one molecule intercalates within the cleft of an adjacent molecule. The two molecules involved in this solid state dimer appear to be stabilised by weak C-H $\cdots$  $\pi$  ( $D_{\text{H}-\pi(\text{centroid})} = 2.62 \text{ \AA}$ ) and offset  $\pi$ -stacking interactions<sup>28</sup> ( $D_{\pi(\text{centroid})-\pi(\text{centroid})} = 4.00 \text{ \AA}$ ). The latter is reasonable as pyrimidine has a reasonably large dipole moment and in the A-type crystal, these dipoles are in an antiparallel orientation adding an additional electrostatic stabilization to the  $\pi$ -stacking. In contrast, **16a** (as well as **14c**) crystallise into the more elongated isomer B, contrary to the solution preference. In this case the broad cleft of one molecule encompasses the bullvalene core structure of an adjacent molecule. Curiously, no dominating intermolecular interactions appear to account for the stability of this crystal form despite its deviation from the preferred solution isomer; a bullvalene C-H $\cdots$ F contact ( $D_{\text{H}-\text{F}} = 2.48 \text{ \AA}$ ) appears to be the most significant contact.

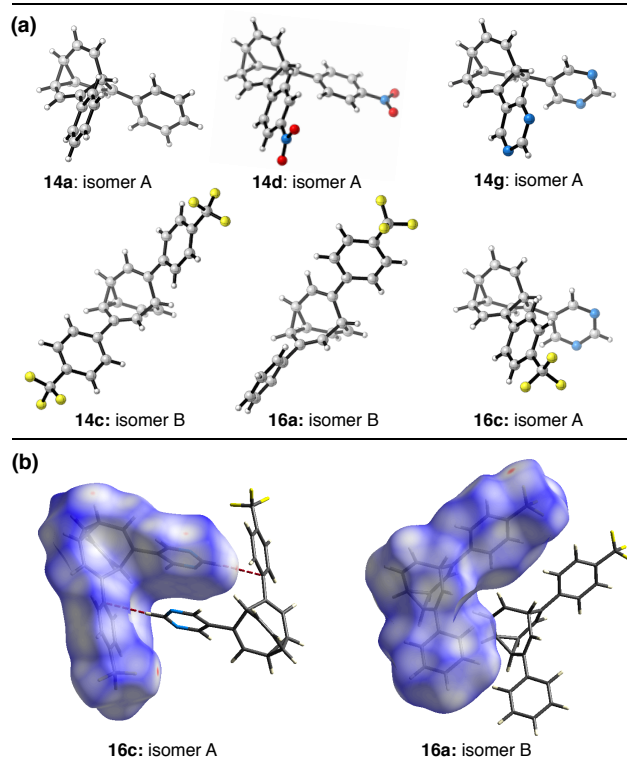


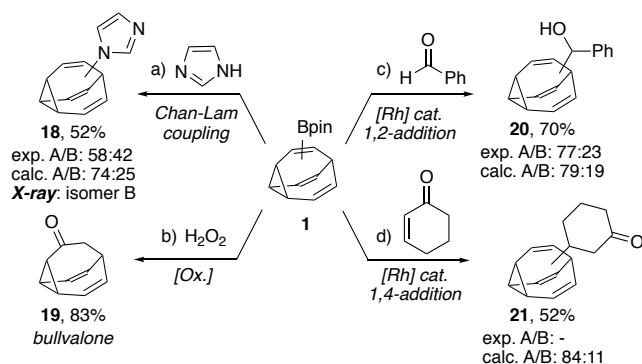
**Figure 3.** (a) Single crystal X-ray structures of diarylbullvalenes. (b) Hirshfeld surface analysis. Single crystal X-ray structures of diarylbullvalenes (grey – C, white – H, blue – N, red – O, and yellow – F). Hirshfeld surface analysis for **16c** and **16a** with selected contacts highlighted. Regions of close contact significantly closer than the sum of their respective van der Waals radii are shown in red.

Disubstituted bullvalenes **2**, **14a**, **14d**, and **14g** all crystallise in the V-shaped isomer A, for which only **14a** (phenyl substituents) and **14g** (pyrimidine) adopt the

intercalated dimer arrangement seen for **16c**. Presumably isomer A in **2** and **14d** are prevented from close approach due to steric bulk and lack of an acidic CH for a weak C-H... $\pi$  contact, respectively. **16a** and **14c** are particularly intriguing as they adopt the isomer B structure in the solid state with no specific intermolecular contacts. Diphenylbullvalene **14a** exhibits polymorphism between our single crystal structure, and that previously recorded by Echavarren.<sup>29</sup> Both structures are in the V-shaped isomer A, yet differ in the relative orientation of one of the phenyl groups. Consequently, our structure of **14a** adopts the intercalated dimer arrangement whereas Echavarren's does not.

The intriguing crystallisation behaviour of substituted bullvalenes prompted us to holistically explore the packing arrangements computationally. For all di- and tri-substituted bullvalene crystal structures, the Hirshfeld surfaces<sup>30,31</sup> were calculated. This analysis highlights regions where intermolecular distances are significantly closer than the sum of their respective van der Waals radii. The results are illustrated for compounds **16c** and **16a** (Figure 3b). Aside from the interactions noted above, only weak intermolecular interactions govern the packing. This conclusion is supported by DFT modelling (CE-B3LYP\*\*) of the intermolecular interaction energies for clusters of bullvalenes **2**, **14a**, **14c**, **14d**, **14g**, **16a**, **16c**, and **17**.<sup>31</sup> In all cases, the total interaction lattice energy is dominated by the dispersion energy contribution (see SI for full details). Spontaneous resolution of these ensembles in the crystal lattice appears to be governed by general shape-selectivity, which can override the inherent thermodynamic preferences observed in solution.

**Scheme 4. Miscellaneous reactions of bullvalene 1<sup>a</sup>**



<sup>a</sup>Reagents and conditions: (a) imidazole (2.0 eq), Cu(OAc)<sub>2</sub> (1.0 eq), B(OH)<sub>3</sub> (2.0 eq), powdered 4Å mol sieves, MeCN, 80 °C. (b) NaOH(aq), H<sub>2</sub>O<sub>2</sub>, THF, EtOH, 0 °C. (c) Benzaldehyde (1.2 eq) KHF<sub>2</sub> (1.2 eq), [Rh(COD)Cl]<sub>2</sub> (1 mol%), dioxane, water, 80 °C. (d) 2-cyclohexen-1-one (1.1 eq) DIPEA (1.0 eq), 2-methylpropane-1,3-diol (1.1 eq), [Rh(COD)Cl]<sub>2</sub> (1 mol%), heptane, methanol, water, 80 °C. Single-point DFT calculations performed at B3LYP-D3BJ/Def2-TZVPPD/CPCM solvent (chloroform) in Orca.

Returning to the synthetic implications of this study, we wished to demonstrate the general utility of building blocks **1-4** beyond the scope of Suzuki cross-coupling reactions. Mono-Bpin-bullvalene **1** was subjected to a

selection of transformations (Scheme 4). Chan-Lam cross-coupling with imidazole furnishes bullvalene **18**.<sup>32</sup> Simple oxidation with hydrogen peroxide smoothly gives bullvalone **19**.<sup>33</sup> Rhodium-catalysed 1,2- and 1,4-addition reactions to benzaldehyde and cyclohexenone gives bullvalenes **20** and **21**, respectively.<sup>34</sup> Despite their attachment to a constantly metamorphosing core structure, the reactivity of the pinacol boronate ester appears to be robust and reliable.

In summary, this work provides the first practical and general synthetic platform to prepare mono-, di-, and tri-substituted bullvalenes. Our boronate ester bullvalenes **1-4** are easy to make and have predictable reactivities. Bpin-B<sub>MIDA</sub>-bullvalene **3** is an effective linchpin enabling the logical synthesis of differentially disubstituted bullvalenes. We hope that these methods will spur further research and applications based on this most enigmatic hydrocarbon.

## Funding Sources

We gratefully acknowledge the New Zealand Royal Society (Marsden Fund No. 15-MAU-154). Calculations were performed using the supercomputing infrastructure of the Computing Center of the Slovak Academy of Sciences acquired in project ITMS 26230120002 and 26210120002 supported by the Research & Development Operational Programme funded by the ERDF. LFP is grateful for the support from the Slovak Research and Development Agency (grant No. APVV-15-0105) and the Scientific Grant Agency of the Slovak Republic (grant No. 1/0777/19). CJS acknowledges the Australian Research Council for equipment provided under grant LE0989336.

## References

- (1) (a) H. Hopf, *Classics in Hydrocarbon Chemistry*, Wiley-VCH, Weinheim, **2000**. (b) G. A. Olah, Á. Molnár, *Hydrocarbon Chemistry, 2nd Edition*, Wiley-VCH, Weinheim, **2003**.
- (2) von E. Doering, W.; Roth, W. R. *Tetrahedron* **1963**, *19*, 715–737.
- (3) Zimmerman, H. E.; Grunewald, G. L., *J. Am. Chem. Soc.* **1966**, *88*, 183–184.
- (4) (a) Barborak, J. C.; Daub, J.; Follweiler, D. M.; Schleyer, P. von R. *J. Am. Chem. Soc.* **1969**, *91*, 7760–7761. (b) Ahlberg, P.; Harris, D. L.; Winstein, S. *J. Am. Chem. Soc.* **1970**, *92*, 4454–4456.
- (5) For a recent review, see: Ferrer, S.; Echavarren, A. M. *Synthesis* **2019**, *51*, 1037–1048.
- (6) (a) Schröder, G. *Angew. Chem. Int. Ed. Engl.* **1963**, *2*, 481–482. (b) Schröder, G. *Angew. Chem.* **1963**, *75*, 722–722. (c) Schröder, G. *Chem. Ber.* **1964**, *97*, 3140–3149.
- (7) (a) Schröder, G.; Merenyi, R.; Oth, J. F. M. *Tetrahedron Lett.* **1964**, 773–777. (b) Oth, J. F. M.; Merényi, R.; Engel, G.; Schröder, G. *Tetrahedron Lett.* **1966**, *7*, 3377–3382.
- (8) Ferrer, S.; Echavarren, A. M. *Angew. Chem. Int. Ed.* **2016**, *55*, 11178–11182.
- (9) (a) Lippert, A. R.; Keleshian, V. L.; Bode, J. W. *Org. Biomol. Chem.* **2009**, *7*, 1529–1532. (b) Lippert, A. R.; Naganawa, A.; Keleshian, V. L.; Bode, J. W. *J. Am. Chem. Soc.* **2010**, *132*, 15790–15799. (c) He, M.; Bode, J. W. *PNAS.* **2011**, *108*, 14752–

14756. (d) Larson, K. K.; He, M.; Teichert, J. F.; Naganawa, A.; Bode, J. W. *Chem. Sci.* **2012**, *3*, 1825–1828. (e) He, M.; Bode, J. W. *Org. Biomol. Chem.* **2013**, *11*, 1306–1317.
- (10) For recent reviews, see: (a) Rowan, S. J.; Cantrill, S. J.; Cousins, G. R. L.; Sanders, J. K. M.; Stoddart, J. F.; *Angew. Chem. Int. Ed.* **2002**, *41*, 898–952. (b) Corbett, P. T.; Leclaire, J.; Vial, L.; West, K. R.; Wietor, J.-L.; Sanders, J. K. M.; Otto, S.; *Chem. Rev.* **2006**, *106*, 3652–3711. (c) Jin, Y.; Yu, C.; Denman, R. J.; Zhang, W.; *Chem. Soc. Rev.* **2013**, *42*, 6634–6654.
- (11) Teichert, J. F.; Mazunin, D.; Bode, J. W. *J. Am. Chem. Soc.* **2013**, *135*, 11314–11321.
- (12) Yahiaoui, O.; Pašteka, L. F.; Judeel, B.; Fallon, T. *Angew. Chem. Int. Ed.* **2018**, *57*, 2570–2574.
- (13) (a) Achard, M.; Mosrin, M.; Tenaglia, A.; Buono, G. *J. Org. Chem.* **2006**, *71*, 2907–2910. (b) D'yakonov, V. A.; Kadikova, G. N.; Dzhemileva, L. U.; Gazizullina, G. F.; Ramazanov, I. R.; Dzhemilev, U. M. *J. Org. Chem.* **2017**, *82*, 471–480.
- (14) For reviews, see: (a) Gandeepan, P.; Cheng, C.-H. *Acc. Chem. Res.* **2015**, *48*, 1194–1206. (b) Hess, W.; Treutwein, J.; Hilt, G. *Synthesis* **2008**, *2008*, 3537–3562. (c) Röse, P.; Hilt, G. *Synthesis* **2016**, *48*, 463–492.
- (15) The catalytic system used in Hilt's [4+2] cycloadditions of alkynyl boronate esters is analogous to the catalytic system reported in [6+2] cycloadditions. For selected works by Hilt see: (a) Hilt, G.; Smolko, K. I. *Angew. Chemie Int. Ed.* **2003**, *42*, 2795–2797. (b) Hilt, G.; Lüers, S.; Smolko, K. I. *Org. Lett.* **2005**, *7*, 251–253. (c) Auvinet, A.-L.; Harrity, J. P. A.; Hilt, G. *J. Org. Chem.* **2010**, *75*, 3893–3896.
- (16) Mono-Bpin-acetylene **6** and bis-Bpin-acetylene **7** are both commercially available. See the SI for details on their preparation.
- (17) The use of alkynyl boronate esters, in particular bis-Bpin-acetylene **7**, under these cobalt-catalysed reaction conditions was initially capricious and required extensive optimisation. We found that stringent purification and drying of all of the reaction components is necessary in order to suppress proto-deborylation of the substrate (see SI for full details). Proto-deborylation of bis-Bpin-acetylene **7** in a Co<sup>I</sup> catalysed [2+2+2] cycloaddition has been reported, see: Iannazzo, L.; Vollhardt, K. P. C.; Malacria, M.; Aubert, C.; Gandon, V. *Eur. J. Org. Chem.* **2011**, *2011*, 3283–3292.
- (18) This reaction was selective for mono-condensation.
- (19) Williams, J. D.; Nakano, M.; Gérardy, R.; Rincón, J. A.; de Frutos, Ó.; Mateos, C.; Monbaliu, J.-C. M.; Kappe, C. O. *Org. Process Res. Dev.* **2019**, *23*, 78–87.
- (20) Stille couplings of triflate substituted bullvalene have been reported by Echavarren, see ref 8.
- (21) Gillis, E. P.; Burke, M. D. *Aldrichimica Acta* **2009**, *42*, 17–27.
- (22) Rebsamen, K.; Röttele, H.; Schröder, G. *Chem. Ber.* **1993**, *126*, 1429–1433.
- (23) Yahiaoui, O.; Pašteka, L. F.; Blake, C. J.; Newton, C. G.; Fallon, T. *Org. Lett.* **2019**. DOI:10.1021/acs.orglett.9b03737.
- (24) Low temperature NMR measurements were made at -60 °C. In some cases, population analysis was precluded due to poor solubility (**3**, **14d**), or severe signal overlap and/or restricted single bond rotation effects (**14b**, **15**, **21**).
- (25) Bismillah, A. N.; Sturala, J.; Chapin, B. M.; Yufit, D. S.; Hodgkinson, P.; McGonigal, P. R. *Chem. Sci.* **2018**, *9*, 8631–8636.
- (26) Echavarren reported the single X-ray crystal structure of **13a** (CCDC 1487024), see ref 8.
- (27) To guard against the possibility that single crystal structures might not reflect the bulk solid phase isomer preference, we recorded powder X-ray diffraction (PXRD) data for compounds **2**, **2** rapidly precipitated, **14c**, **14d**, **16a**, and **16c**. Experimental data closely matches patterns simulated from the single crystal structures (see SI for full details).
- (28) Martinez, C. R.; Iverson, B. L. *Chem. Sci.* **2012**, *3*, 2191–2201.
- (29) For Echavarren's crystal structure of **14a** (CCDC 1487025), see ref 8.
- (30) (a) Spackman M. A.; Jayatilaka, D. *CrystEngComm*, **2009**, *11*, 19. (b) Spackman, M.A.; McKinnon, J.J.; *CrystEngComm*, **2002**, *4*, 378-392
- (31) All calculations were performed using the *CrystalExplorer* software package, version 17.5. <http://crystalexplorer.scb.uwa.edu.au> (last accessed 22/11/2019)
- (32) Vantourout, J. C.; Miras, H. N.; Isidro-Llobet, A.; Sproules, S.; Watson, A. J. B. *J. Am. Chem. Soc.* **2017**, *139*, 4769–4779.
- (33) This 3-step procedure constitutes the shortest synthesis of bullvalone to date. For the original work on bullvalone, see: W. von E. Doering, W.; Ferrier, B. M.; Fossel, E. T.; Hartenstein, J. H.; Jones, M.; Klumpp, G.; Rubin, R. M.; Saunders, M. *Tetrahedron*, **1967**, *23*, 3943–3963.
- (34) (a) Zhang, C.; Yun, J. *Org. Lett.* **2013**, *15*, 3416–3419. (b) Simmons, E. M.; Mudryk, B.; Lee, A. G.; Qiu, Y.; Razler, T. M.; Hsiao, Y. *Org. Process Res. Dev.* **2017**, *21*, 1659-1667.